

Pedestrian Walking Direction from Video

Slimane Larabi*, Amina Bensebaa*

*Computer Science Department, USTHB University, Algeria

Keywords: Pedestrian direction, Video, Motion, Silhouette, Vanishing point

Abstract

In this paper we consider direction estimation of pedestrian motion. The idea is to base estimation on image sequence analysis, where the detection of the head and toe points provide measurements for vanishing point estimation (roughly, these points move along parallel lines in 3D, when the direction of walk is fixed). For each frame, the top and the bottom points of the segmentation are extracted. One line is fitted to the collection of top points and one to the collection of the bottom points. Given these two lines, the vanishing point is estimated and from this the direction of the pedestrian. Experiments conducted on database available in public demonstrate the efficiency and robustness of the proposed method. Obtained results are compared to the state of the art and discussed.

1 Introduction

Estimating direction of pedestrians walking or running from video could be very useful for many applications: video surveillance, pedestrian protection using driver assistance systems, traffic control systems, improving people tracking and identification systems, accident avoidance system for smart cars. Many contributions have been proposed and the challenge remains due to external conditions that degrade the images quality especially for low resolution images.

In this paper we address the task of estimating direction of moving pedestrians. The scene is depicted by a series of images taken by a single camera. Movements of head and feet of pedestrian's silhouette serve for determining the direction of movement of that person. Each movement (top and bottom) is described by a line. In order to be robust against the small individual movements of the head and the feet, the positions of the head and feet, respectively, are fitted to a top and a bottom line via linear regression. According to projective geometry, these lines, that are parallel in 3D, intersect in a vanishing point. Using the estimated vanishing point, the principal point coordinates and the focal length, the direction of the movement of the person is determined.

We begin this paper by presenting the related works. The section 3 is devoted to the principles of our approach. In section 3.5 we explain how the proposed algorithm is adapted to face to complex scenes and multiples trajectories. We present the conducted experiments on available datasets and we discuss the

obtained results in section 4. We conclude this paper by some suggestions for improving the proposed method.

2 Related Works

The majority of works devoted to pedestrian direction estimation use classification methods and deliver a rough direction of the body. Support Vector Machine (SVM) based scheme has served in [2] to estimate the walking direction of pedestrian from images where 90% of correct recognition is obtained for 16 directions. It has used also in [8] to estimate the discrete probability distribution of the orientation. This approach was trained with the INRIA pedestrian dataset and results of tests in realistic conditions show that 49.7% fall in same bin as ground truth and 81.3% fall in same or adjacent bins. Chen [15] use sparse representation technique on each frame for body pose classification, generating (noisy) observation on body poses which is improved by soft coupling of body pose with the movement in a particle filtering framework. For the 8 directions considered, 75% as pose accuracy is achieved. Guangzhe [6] estimate the pedestrian orientation using Adaboost as a classifier and achieve 64% accuracy for 8 orientations. In [16], D. Baltieri estimate person orientation on single images based on appearance features. The three level HoG feature set is extracted from each people detection and provided as input to an array of binary classifiers trained on a set of discrete orientations. An average of 70% is obtained for classification of 8 directions. Tao and Klette [4] proposed novel Random Decision Forests to simultaneously classify pedestrians and their directions and yield results comparable to those of state-of-the-art and baseline methods. In [7], authors present an approach for the joint probabilistic estimation of pedestrian head and body orientation in the context of intelligent vehicles. Quantitative experiments showed that joint tracking of head and body decreases the angular mean error for head/body orientation by $13^\circ/10^\circ$ compared to single frame estimation and further by $3^\circ/2^\circ$ compared to independent tracking. A novel approach for jointly estimating head, body orientations is proposed in [11]. Target feet positions are estimated with the multi-target tracking approach and used for head localization and cropping via a 3D head-plus-shoulder model registered through shape matching, the precision 0.87 is achieved. H. Liu and L. Ma [17] estimate the orientation based on online appearance-based classifier update. Reliable motion direction is determined acting as pre-estimated person orientation to update the appearance-based classifier. This approach achieves more competitive performances especially for unknown scenes. R. Raman [13] pro-

pose an approach for direction estimation of a moving pedestrian estimation. The dimensional change-based feature is used to estimate the direction of motion; eight discrete directions of motion are considered and the hidden Markov model is used for classification, 90% of accuracy is achieved on CASIA-B dataset [1].

Projective geometry can help to solve this problem. Many works have dealt with pedestrians motion for camera calibration. The horizon line is estimated by observing the human motion in different directions. Authors exploit the fact that the line joining the head positions of a pedestrian at two time instances is parallel to the line joining the feet (or bottom) positions at these same corresponding time instances. Similarly, the line joining the head to the feet in a frame is parallel to the line joining the head to feet the next frame.

Using frames of a pedestrian walking in a straight line, authors in [3], recover three orthogonal vanishing points for camera calibration method. To do this, authors assume that shoes follows periodic motion.

The published works related to vanishing points and lines are devoted to camera calibration and then either assume accurate positions of pedestrian's points, or propose a rough detection and then an approximation of the points.

In [3] left and right toes of the shoes are extracted from the pedestrian blobs when the two legs are maximally separated and used to construct two image lines. Obtaining such frames is unrealistic in real world: the presence of toes is not guaranteed, foot may be occluded or not separated from the other, and the distance separating the foot is different.

Authors in [10] calculate top and bottom locations from the tracked pedestrians using the center of mass and the second order moment of the lower and the upper portion of the bounding box of the foreground region. In [18], the bottom point determined either as the end point of the major axis of the ellipse fitting the pedestrian's blob or the end of line fitting the bounding box. These two methods [10] [18] do not locate specific point of foot and then we can't assert that the pair of lines joining respectively two successive top points and bottom points are parallel in 3D.

In this paper our aim is to improve the results of the state of the art. Our contributions are multiple:

- Directions in the scene are mapped on the image plane such that to each direction is associated a bounded area. The area of appartaining of vanishing point indicates the walking direction.
- Easiness of direction computation so as the inference of direction change directly from the evolution of vanishing points on the mapped areas on image plane.
- With a certain delay (30 frames) we surpass the best results of the state of the art obtained for CASIA-A and CASIA-B.

3 Proposed Approach

3.1 Walking Direction of Pedestrians from 3D to 2D

Let $\omega(u_\omega, v_\omega)$ be the vanishing point located on the image plane associated to the direction of $((\Delta^h), (\Delta^f))$ defined by

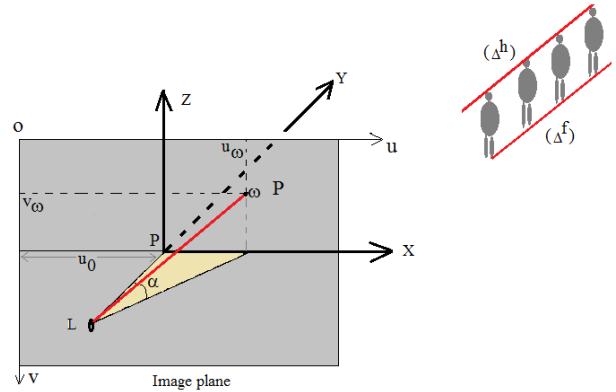


Figure 1. Vanishing points ω associated to the direction of $((\Delta^h), (\Delta^f))$.

pedestrian bodies parts (head and feet) along the motion trajectory (see figure 1). We will consider the pedestrian's direction as the value of the angle α relatively to the axis PY , where $(PXYZ)$ is the associated camera reference. The value of α is computed using ω , the focal length f and the u -coordinates of the principal point $P(u_0, v_0)$ as follow:

$$\alpha = \arctan\left(\frac{u_\omega - u_0}{f}\right) \quad (1)$$

3.2 Determining the values of u_0 and f

The values of u_0 and f , needed for calculating α angle, may be available either:

- Camera calibration,
- Parameters evaluation by performing a leaning stage using at least two pairs of parallel lines having two known different directions α_1, α_2 giving two vanishing points ω_1, ω_2 in image plane. The values of u_0, f are computed as follow.

$$\tan(\alpha_1) \times f = u_{\omega_1} - u_0 \quad (2)$$

$$\tan(\alpha_2) \times f = u_{\omega_2} - u_0 \quad (3)$$

If $\alpha_1 \neq 0$ and $\alpha_2 \neq 0$, the values of f, u_0 are estimated by solving the system of linear equations (2) and (3).

3.3 Finding pair of parallel 3D lines in the scene

Images of walking pedestrian contain geometric features useful for inferring information about 3D scene, especially features related to projective geometry assuming that image may be considered as perspective projection of the 3D scene.

If we look at figure 2, we can see that when pedestrian moves from one position to another on the same ground, the two lines defined by the limits of the heads and the limits of feet may be considered as parallel to the ground [9][10]. In the image plane, their projections (δ^h, δ^f) intersect at the vanishing point ω .

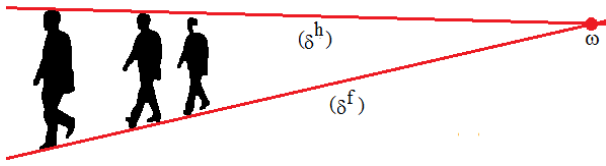


Figure 2. Images of the parallel lines in 3D giving the vanishing point in 2D

In theoretical case, joining the bottom points of pedestrian's images will define a line if they correspond to same 3D point of pedestrian's feet. This is an unrealistic situation, because feet in 3D is moving and then the bottom points are unmatched points (see figure 2). In the same case, head pose may change. Consequently, in image the two lines will be determined by minimizing the distance from the extremities (top, bottom) to the considered line (the best-fitting linear regression model). Note that more are numerous the used silhouettes in this process, more is the accuracy of fitted line in image.

3.4 Direction computation from images sequence: Algorithm

The first step (Learning stage) is the computation of camera parameters (f, u_0) using two set of frames corresponding to the motion of the pedestrian in two different directions. In order to get best values of f, u_0 , we will take more than 2 directions. More details are given in experimental results. Once the parameters f, u_0 are estimated, we compute the direction for each new frame using the equation 1 (Testing stage).

The Naive Algorithm

Begin

$F_i, i = 0..k$ are the frames to be processed
Focal length (f) and u-coordinate of the principal point (u_0) are computed in the learning stage

Start step:

- $i = 0$ # the order number of the starting frame
- Locate the top points p_0^h, p_1^h and bottom points p_0^f, p_1^f of the pedestrian's silhouette for the frames F_0, F_1
- Fit via linear regression the top points to line Δ^h , and the bottom points to line Δ^f .
- Compute the vanishing point $\{\omega\} = \Delta^h \cap \Delta^f$
- Compute the direction $\alpha = \arctan((u_\omega - u_0)/f)$.
- # α is the estimated direction for the frames F_0, F_1

Next step:

- $i=2$

For each $F_i, (i = 1..k)$

Do

1. Locate the top point p_i^h and bottom point p_i^f of the silhouette
2. Fit via linear regression the top points $p_k^h (k=0..i)$ to new line Δ^h
3. Fit via linear regression the bottom points $p_k^f (k=0..i)$ to new line Δ^f

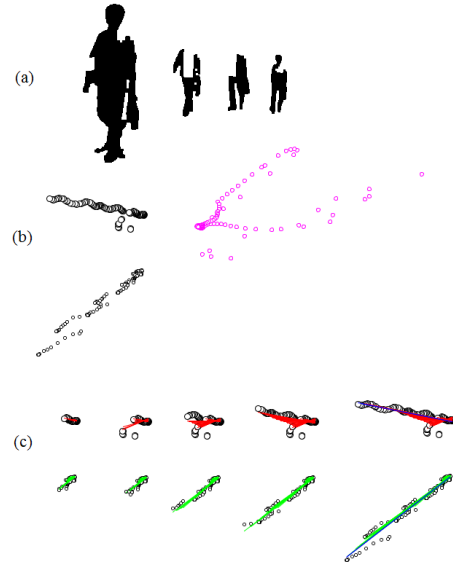


Figure 3. (a) Sample of silhouettes from used video. (b) Located top and bottom points of silhouettes (black circles) and computed vanishing points (magenta circles) applying the naive algorithm. (c) Evolution of the fitted lines joining top (red color) and bottom points (green color).

4. Compute the vanishing point $\{\omega\} = \Delta^h \cap \Delta^f$
 5. Compute the value of $\alpha = \arctan((u_\omega - u_0)/f)$
- # α is the estimated direction for the frame F_i
EndFor
End.

For a video sequence of direction 18° taken from Casia-B dataset, we show in figure 3 sample of processed silhouettes and the extracted reference (top, bottom) points. Due to head occlusion and error of segmentation, the reference points are not aligned. The evolution of the lines fitting is illustrated where we can see that these errors change the allure of fitted lines and consequently many computed vanishing points are far from the correct position (see figure 3(b)).

3.5 Adapting the method for complex scenes

It is clear that if we use all frames to determine the lines fitting the top and bottom points, the intersection point (vanishing point) is sensible to occlusion, segmentation error, direction change and non planar ground. We can see in figure 4 that head of pedestrians are missing from frames 46 – 55 due to occlusion, the top points in this case are taken from shoulders. The previous fitted line for top points becomes far from the new top points.

However, instead to consider for the current frame all previous frames, we consider only the previous ones such that the slope is approximatively stable for the new fitted line. We verify if the located top point is near from the fitted line for the previous frames, then the current frame will be included in the fitting of the new line. Otherwise, the current frame will be

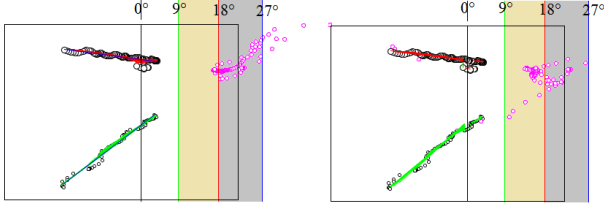


Figure 4. Vanishing points computed applying the naive algorithm (Left) and improved algorithm (right)

considered as first one of a new fitting process. This will, in case of missing parts of silhouette (example head) allows to get good estimation, because the top points will define a line which is approximatively parallel to bottom line. Figure 4 illustrates how the fitted lines are corrected giving more better results.

The new Algorithm and Complexity

The New Algorithm

Begin

$F_i, i = 0..k$ are the frames to be processed

Focal length (f) and u-coordinate of the principal point (u_0) are computed in learning stage

- $i_{start} = 0$ # the order number of the starting frame

- *start_again*:

```

{
-  $i = i_{start}$ 
- Locate the top points  $p_i^h, p_{i+1}^h$  and bottom points  $p_i^f, p_{i+1}^f$  of the pedestrian's silhouette for the frames  $F_i, F_{i+1}$ 
- Fit via linear regression the top points to line  $\Delta^h$ , and the bottom points to line  $\Delta^f$ .
- Compute the vanishing point  $\{\omega\} = \Delta^h \cap \Delta^f$ 
- Compute the direction  $\alpha = \arctan((u_\omega - u_0)/f)$ .
#  $\alpha$  is the estimated direction for the frames  $F_i, F_{i+1}$ 
-  $i=i+2$ 
}

```

For each $F_j, (j = i..k)$

Do

1. Locate the top points p_j^h and bottom points p_j^f of the pedestrian's silhouette

2. **If** (p_j^h is near from Δ^h)

Then Fit via linear regression the top points p_k^h

($k = i_{start}..j$) to new line Δ^h

Else $i_{start} = j$, Goto *start_again*

3. **If** (p_j^f is near from Δ^f)

Then Fit via linear regression the bottom points p_k^f

($k = i_{start}..j$) to new line Δ^f

Else $i_{start} = j$, Goto *start_again*

4. Compute the vanishing point $\{\omega\} = \Delta^h \cap \Delta^f$

5. Compute the value of $\alpha = \arctan((u_\omega - u_0)/f)$.

α is the estimated direction for the frame F_j

EndFor

End.

The complexity of the algorithm is $O(mk)$, it depends on

m (the number of pixels of outline silhouette) and on k (the number of frames). If we consider that $m \approx n$, where $n \times n$ defines the image size, then the complexity is $O(n)$.

4 Experimental Results

We used several datasets with different environments, several walk direction, various resolution provided by CASIA-A (binary, outdoor), CASIA-B (Binary, indoor).

Dataset CASIA-A [1] includes 20 persons. Each person has 12 image sequences, 4 sequences for each of the three directions, i.e. parallel (0), 45 degrees and 90 degrees to the image plane. The length of each sequence depends on the walker's speed and ranges from 37 to 127. The Dataset CASIA-A includes 19139 images.

CASIA-B [1] dataset is composed by 124 groups of silhouettes corresponding to 13640 binary frame sequences with 11 different walk directions ranging 0° to 180° from view axis of camera. Note that pedestrians are carrying bag, wearing coat or having a regular outfit without carrying anything.

4.1 Experimental Setup

For the learning stage, we used only one group (the first one). We computed the parameters (f, u_0) using frames of three known directions 18°, 36°, 54°. For each new frame from images sequence, the two lines best-fitting linear regression model for respectively the top points and bottom points are estimated and the vanishing point is located. This computation process is repeated for all frames, and the vanishing points moves depending on the data (top and bottom points). We selected the ultimate vanishing point and evaluated the two parameters (see figure 5). We note the noisiness of the processed data giving non-aligned top and bottom points. Each pair of directions allows computing the f, u_0 . Their averages for CASIA-B ($f = 325$ pixels, $u_0 = 187$ pixels) are selected for the testing stage. We notice that frames with occluded head are eliminated from used video sequence.

The 123 remaining groups have been used for test and then for each set of frames, the direction is computed following the method described in section 3.

4.2 Accuracy of estimated direction estimation related to the delay

Our first experiment concerns determining pedestrian direction based on video. Process of direction estimation starts after delay (a set of frames of the video are required). The number of these frames is determined such that it allows an accurate estimated direction due to the fitting lines process which need numerous points in order to deliver an accurate line. We studied the accuracy of computed direction related to the delay. Obtained results indicate that:

- 60 frames (3 sec of walking) are sufficient to get an accurate estimation (see figure 6).

- The mean error and standard deviation of the obtained for CASIA-A are greater than of CASIA-B, this is due to the result of outdoor image segmentation giving for many frames

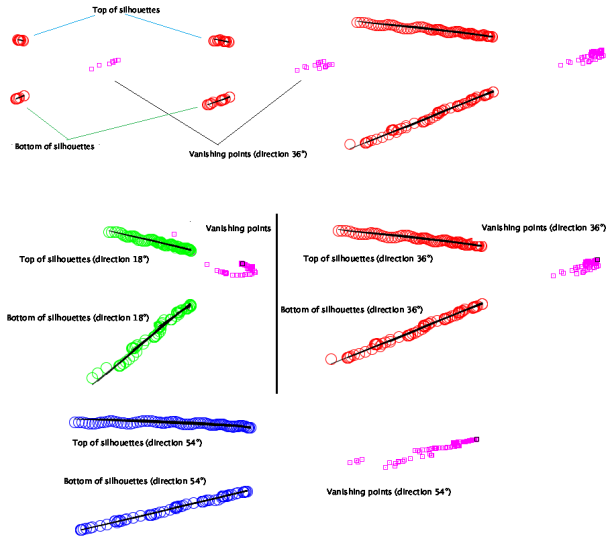


Figure 5. (Top) Evolution of lines joining the top and bottom of silhouettes and vanishing points for direction 36° . (Middle and bottom) Lines are reevaluated for new pairs of points (green, red, blue circles) and new vanishing point are located (magenta squares) for three directions (18° , 36° , 54°).

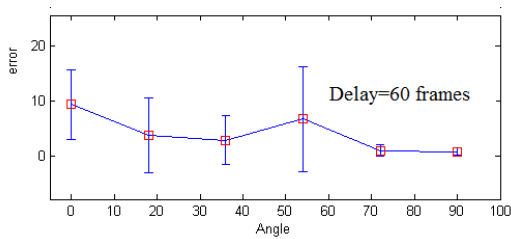


Figure 6. Mean error and standard deviation for the 6 directions of CASIA-B dataset

shadow regions as a part of silhouettes or missing region. The displacement of the top or bottom point located on the head and feet parts will disturb the linear regression fitting process and consequently, the intersection point will more distant from the required vanishing point. The error and standard deviation increase in this case.

- The orientation 0° and 90° constitute the sensitive cases of our method. Indeed, for 0° the bottom pixels of silhouettes are far from their meaning and the fitted line will produce an intersection point far from the true position. For the case 90° , the two fitted lines are theoretically horizontal and the vanishing point must be at infinity. However, in practice, the intersection point may be not very far due to the fact that one or the two fitted lines aren't horizontal.

4.3 Direction estimation: Results and comparison

The estimation of the pedestrian direction from a current frame is based on the previous frames.

Table 1. Confusion matrix for Casia dataset B with delay 0,20, 40 frames. Values A (Accuracy) given are percentages.

d (delay)	d_1, d_2, d_3, d_4, d_5	A	A [13]
d_1 (0 f)	74.8, 5.5, 6.2, 3.1, 10.3	74.8	93
d_1 (20 f)	84, 2, 1.3, 1.9, 10.9	84	
d_1 (40 f)	93.3, 0.5, 0, 0.3, 5.8	93.3	
d_2 (0 f)	0.9, 92, 5.8, 0.8, 0.5	92	91
d_2 (20 f)	0.2, 98.1, 1.6, 0.1, 0	98.1	
d_2 (40 f)	0, 100, 0, 0, 0	100	
d_3 (0 f)	0, 04.2, 95.4, 0.2, 0.2	95.4	88
d_3 (20 f)	0, 01.1, 98.7, 0, 0	98.7	
d_3 (40 f)	0, 0, 100, 0, 0	100	
d_4 (0 f)	0, 0.1, 23.4, 76.4, 0.2	76.4	
d_4 (20 f)	0, 00, 14.6, 85.4, 0	85.4	89.8
d_4 (40 f)	0, 0, 5.7, 94.3, 0	94.3	
d_5 (0 f)	1.9, 1.5, 2.2, 14.7, 79.7	79.7	
d_5 (20 f)	0, 0.2, 0.2, 7.3, 92.2	92.2	92.6
d_5 (40 f)	0, 0, 0, 1.9, 98.1	98.1	
(Our 0 f)	Balanced	83.65	90.87
(Our 20 f)	Accuracy	91.66	
(Our 40 f)		97.15	

4.3.1 Dataset CASIA-B

Due to the linear regression technique used for fitting top points and bottom points, the error of estimation is very large for the first frames as found in the previous subsection. We studied the number of correct estimated direction related to the delay of frames which represent the number of frames non processed at the start. As the interval between the 11 directions is 18° , then if the error is less than 9° the direction estimated is considered as correctly classified. In order to compare our method and [13] we merged the 11 different walk directions of CASIA Dataset B into five discrete directions as made in [13]. We give in table 1 the confusion matrix computed for Casia-B. The average of classification rate (Balanced accuracy) 91.66% surpasses the rate obtained by [13] (90.87%) for a delay equal to 20 frames. With a delay of 40 frames we reach the rate 97.15%.

4.3.2 Dataset CASIA-A

We give in table 2 the confusion matrix computed for Casia-1. The average of classification rate (Balanced accuracy) 96.14% surpasses the rate obtained by [13] (94.58%) for a delay equal to 20 frames. With a delay of 30 frames we reach the rate 98.11%.

5 Conclusion

Starting from a video sequence of a walking pedestrian, we propose a new method for accurate estimation of pedestrian's direction. We can distinguish without ambiguity the pedestrian direction using at least 30 frames (1 second of walk) and we compute with high precision the direction from 60 frames (2 seconds of walk). The obtained results surpass all those ob-

Table 2. Confusion matrix for Casia dataset A with delay 0, 20, 30 frames. Values A (Accuracy) given are percentages

d	d_1, d_2, d_3	A	A [13]
d_1 (Our 0 f) (Our20F) (Our30f)	79.7, 15.9, 4.3 89.2, 10.2, 0.6 94.4, 5.5, 0.02	79.73 89.18 94.4	92.5
d_2 (Our 0 f) (Our 20 f) (Our 30 f)	0.5, 93.2, 6.3 0, 99, 6, 0.04 0, 99, 9, 0.1	93.22 99.56 99.91	92.5
d_3 (Our 0 f) (Our 20 f) (Our 30 f)	1.2, 7.3, 91.5 0, 0.3, 99.7 0, 0, 100	91.5 99.7 100	98.75
(Our 0 f) (Our 20 f) (Our 30 f)	Balanced	88.15 96.14 98.11	94.58

tained in the literature and the proposed approach can serve for real time applications. As future works, we will extend our work in order to:

- Consider a blob (group of pedestrians) instead of a silhouette (one pedestrian),
- Tackle the direction change and the non planarity of the ground,
- Provide correct direction whatever the frame segmentation errors.

References

- [1] S. Yu and D. Tan and T. Tan, A Framework for Evaluating the Effect of View Angle, Clothing and Carrying Condition on Gait Recognition, ICPR, Hong Kong, China. August 2006
- [2] H. Shimizu, T. Poggio., Direction Estimation of Pedestrian from Multiple Still Images. IV 2004
- [3] S. Huang and X. Ying and J. Rong and Z. Shang and H. Zha, Camera Calibration from Periodic Motion of a Pedestrian, CVPR 2016
- [4] J. Tao and R. Klette, Integrated Pedestrian and Direction Classification using a Random Decision Forest, ICCV Workshop 2013, pp. 230-237
- [5] S. Zheng, J. Zhang, K. Huang, R. He, T. Tan, Robust view transformation model for gait recognition, International Conference on Image Processing, Brussels, Belgium, 2011
- [6] Z. Guangzhen, T. Mrutani, S. Kajita, K. Mase, Video based estimation of pedestrian walking direction for pedestrian protection system, Journal of Electronics (China), Vol.29 No.1/2, March 2012
- [7] F. Flohr and M. Dumitru-Guzu and J. F. P. Kooij and D. M. Gavrilu, Joint probabilistic pedestrian head and body orientation estimation, IEEE Intelligent Vehicles Symposium (IV), June 8-11, 2014. Dearborn, Michigan, USA
- [8] T. Gandhi and M. M. Trivedi, Image Based Estimation of Pedestrian Orientation for Improving Path Prediction, IEEE Intelligent Vehicles Symposium, Eindhoven University of Technology Eindhoven, The Netherlands, June 4-6, 2008
- [9] F. Lv and T. Zhao, and R. Nevatia, Self-calibration of a camera from video of a walking human., IEEE International Conference of Pattern Recognition, 2002.
- [10] I. N. Junejo, Using Pedestrians Walking on Uneven Terrains for Camera Calibration., Machine Vision and Applications, January 2011, Volume 22(1)
- [11] E. Ricci and J. Varadarajan and R. Subramanian and S. R. Bulu and N. Ahuja and O. Lanz, Uncovering Interactions and Interactors: Joint Estimation of Head, Body Orientation and F-formations from Surveillance Videos., ICCV 2015.
- [12] R. Raman and P. K. Sa and B. Majhi and S. Bakshi, Acquisition and corpus description of NITR conscious walk dataset., ACM SIGBioinformatics Record, vol. 7, pp. 1, 2017.
- [13] R. Raman and P. K. Sa and B. Majhi and S. Bakshi, Direction Estimation for Pedestrian Monitoring System in Smart Cities: An HMM Based Approach, IEEE Access. 2016 — journal-article. DOI: 10.1109/ACCESS.
- [14] M. Andriluka and S. Roth and B. Shiele, Monocular 3D pose estimation and tracking by detection., IEEE Conf. Comput. Vi. Patter Recognition. (CVPR), June 2010, pp. 623-630.
- [15] C. Chen and A. Heili and J. M. Odobez, 8th IEEE International Conference on Advanced Video and Signal Based Surveillance (AVSS), 2011, pp.5-10., Combined estimation of location and body pose in surveillance video
- [16] Baltieri, D. Vezzani, R. and Cucchira, R. , People orientation recognition by mixtures of wrapped distributions on random trees., In proc. Eur. Conf. Comput. Vis. (ECCV), V 2012, pp. 270-283.
- [17] Liu, H. and Ma, L. , Online person orientation estimation based on classifier update., In Proceeding of IEEE Int. Conf. Image Processing ICIP, Sept, 2015, pp. 1568-1572.
- [18] J. Guan, F. Deboeverie, M. Slembrouck, Extrinsic calibration of camera networks based on pedestrians, Sensors 2016, 16, 654; doi:10.3390/s16050654.
- [19] Asma Bellili, Slimane Larabi, Neil M. Robertson, Outlines of objects detection by analogy , In the LNCS proceedings of 15th on Computer Analysis of Images and Patterns (CAIP'2013), pp. 385-392, August 27-29, York, UK